Electron Paramagnetic Resonance Studies on the High-Salt Form of Bovine Spleen Purple Acid Phosphatase†

M. W. Crowder, J. B. Vincent,‡ and B. A. Averill*

Department of Chemistry, University of Virginia, Charlottesville, Virginia 22901

Received May 15, 1992; Revised Manuscript Received July 13, 1992

ABSTRACT: The EPR spectra of the high-salt form of reduced bovine spleen purple acid phosphatase ($BSPAP_r$) and its complexes with inhibitory tetrahedral oxyanions, AMP, and fluorine have been examined in the 4–30 K temperature range. The EPR spectrum of the high-salt form of $BAPAP_r$ is identical to that previously reported for the low-salt form (Averill et al. (1987) *J. Am. Chem. Soc. 109*, 3760–3767), indicating that the substantial differences in conformation of the two forms result in undetectable alterations in the electronic structure of the binuclear iron center. Phosphate, AMP, and arsenate all result in broadened, highly anisotropic EPR spectra with decreased values of the antiferromagnetic coupling constant, $-2J$, while molybdate and tungstate produce a sharp axial or slightly rhombic spectrum, respectively, and fluoride produces an anomalous spectrum with an inverted **g**-tensor. These results are consistent with binding of the two classes of oxyanions (and AMP) to distinct sites at or near the binuclear iron center, while fluoride binds in yet a third mode. EPR spectra of the $BSPAP_r$ complex with molybdate show altered relaxation behavior in the presence of phosphate, consistent with a 50% decrease in the magnitude of $-2J$, suggesting that phosphate binds to the molybdate complex to produce a ternary complex analogous to that proposed for molybdate inhibition on the basis of kinetics studies.

Purple acid phosphatases (PAP's)[1] are a class of phosphoprotein phosphatases that catalyze the hydrolysis of nucleotide di- and triphosphates, phosphoamino acids, and aryl phosphates (Vincent & Averill, 1990). The two most thoroughly studied examples, those from porcine uterine fluid (uteroferrin, Uf) and bovine spleen (BSPAP), have been examined by a wide array of spectroscopic and physical techniques, including UV–visible, resonance Raman, NMR, EPR, ENDOR, EXAFS, and Mössbauer spectroscopy and direct magnetic susceptibility measurements (summarized in Antanaitis & Aisen, 1983; Doi et al., 1988a; Que & True, 1990; and Vincent et al., 1990). These studies have established the existence of a novel binuclear μ-oxo- (hydroxo-) bridged iron center that can exist in two interconvertible forms: (1) an oxidized, purple, essentially inactive form containing two high-spin ferric ions antiferromagnetically coupled to give an $S = 0$ ground state (PAP_o) and (2) a reduced, pink, catalytically active form containing an antiferromagnetically coupled Fe(III)–Fe(II) center with an $S = {}^1/_2$ ground state (PAP_r). The most salient results are the following: PAP_r exhibits a distinctive EPR signal at $g < 2$ below 30 K, while resonance Raman spectra have demonstrated that the intense color of PAP's is due to a tyrosinate to Fe(III) charge transfer transition (Antanaitis et al., 1982; Averill et al., 1987; Gaber et al., 1979). EXAFS studies on $BSPAP_o$ (Kauzlarich et al., 1986) and Uf_o (Que & Scarrow, 1988) have demonstrated the presence of an Fe---Fe separation of 3.0–3.2 Å, which increases to ca. 3.5 Å in Uf_r (True & Que, 1990). Direct magnetic susceptibility (Antanaitis et al., 1983; Averill et al., 1987; Davis et al., 1982, Day et al., 1988; Doi et al., 1987; Mockler et al., 1983; Sinn et al., 1983), variable-temperature NMR (Lauffer et al., 1983; Scarrow et al., 1990; Wang et al., 1992), and EPR (Antanaitis & Aisen, 1983; Averill et al., 1987), and ^{57}Fe Mössbauer studies (Debrunner et al., 1983) suggest that the antiferromagnetic exchange interaction ($2J$, for the spin Hamiltonian $H = -2JS_1 \cdot S_2$) between the iron atoms is much stronger in PAP_o ($-2J$ = 80–300 cm^{-1}) than in PAP_r ($-2J$ = 10–22 cm^{-1}).

Given the existence of such detailed spectroscopic information on the resting forms of the PAP's, the changes in spectroscopic properties elicited upon binding of inhibitors, such as tetrahedral oxyanions that are potential substrate or product analogs, might be expected to provide information on whether and how the binuclear iron center participates in the catalytic mechanism. On the basis of such studies, several groups have indeed proposed catalytic mechanisms involving the diiron center (David & Que, 1990; Dietrich et al., 1991; Vincent et al., 1992a,b). Only recently, however, has it been demonstrated through combined spectroscopic and kinetics (Vincent et al., 1991a, 1992a; Pyrz et al., 1986) and electrochemical (Wang et al., 1991) studies that there appear to exist two distinct binding sites for tetrahedral oxyanions: one at the substrate binding site that results in competitive inhibition, red shifts of λ_{max} of PAP_r at low pH, and a broadened rhombic EPR signal that is very temperature- and power-sensitive, and induces oxidation of the mixed-valence binuclear center, and another site that results in noncompetitive inhibition, a blue shift in λ_{max} of PAP_r, and a sharp axial EPR signal and stabilizes the mixed-valence center to aerobic oxidation. Larger oxyanions such as molybdate and tungstate bind only to the latter site, while phosphate and arsenate bind to the former site with a higher affinity than to the latter. In addition, evidence has recently been obtained for the existence of a covalent phosphoryl-enzyme intermediate, E-PO_3^{2-}, in the catalytic mechanism (Vincent et al., 1991b). A mechanistic hypothesis that is consistent with the published data has been proposed (Vincent et al., 1992a) and suggests that

† This work was supported by NIH Grant GM 32117 to B.A.A. and by NIH Postdoctoral Fellowship GM 13500 to J.B.V.

* To whom correspondence should be addressed.

‡ Current address: Department of Chemistry, University of Alabama, Tuscaloosa, AL 35487.

[1] Abbreviations: PAP, purple acid phosphatase; Uf, uteroferrin; BSPAP, bovine spleen purple acid phosphatase; subscripts o and r, diferric and mixed-valence forms of the enzymes; MES, 2-(*N*-morpholino)-ethanesulfonic acid.

0006-2960/92/0431-9603$03.00/0

molybdate and tungstate inhibit by complexing to the E-PO_3^{2-} intermediate to give a species such as E-PO_3^{2-}·MoO_4 (**1**).[2] Direct detection of an intermediate such as **1** under steady-state conditions is likely to be difficult, but one might expect that it would be possible to form ternary complexes analogous to **1**, such as an E·PO_4·MoO_4 species in which both oxyanion binding sites are occupied simultaneously. The present paper

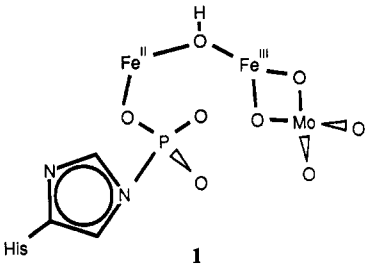

1

describes the EPR spectra of complexes of $BSPAP_r$ with inhibitory tetrahedral oxyanions and fluoride (a potential hydroxide analog) and reports spectroscopic evidence suggesting formation of a ternary complex.

MATERIALS AND METHODS

Instrumentation. EPR spectra were collected on a Bruker ESR 300 spectrometer equipped with an Oxford ESR 900 continuous-flow cryostat and an Oxford Model ITC 4 temperature controller. Operating temperatures were read directly from the controller, which was calibrated with a carbon glass sensor. Protein concentrations were determined using an HP8452-A diode array UV–vis spectrophotometer or a Beckman DU spectrophotometer equipped with a Gilford Model 252-D accessory, using $\epsilon_{536} = 4000$ L/(mol·cm) (Vincent et al., 1991a).

Methods. The high-salt form of bovine spleen purple acid phosphatase was isolated according to previously published procedures (Vincent et al., 1991a). For variable pH studies, the protein was dialyzed against 0.1 M acetate buffer (pH 4.25 and 5.0) or 0.1 M MES buffer (pH 6.0). To probe specific buffer effects, pH dependence studies were also conducted in 0.1 M MES buffer (pH 4.25, 5.0, 6.0, and 7.0); all buffers contained 2 M KCl. Samples at pH 7.0 were made by 10 successive 10:1 dilution/concentration cycles using a Centricon 10 with 0.1 M HEPES or 0.1 M MES buffer pH 7.0; the protein samples were then concentrated to ca. 16 mg/mL using the Centricon 10. The $BSPAP_r$ complexes with PO_4, AMP, AsO_4, and F^- were made by adding 15 μL of the inhibitor stock at pH 5.0 to the 500-μL sample to give a final concentration of 10–50 times K_i. The samples were incubated at room temperature for ca. 20 min, loaded into 4-mm o.d. quartz EPR tubes, and then frozen by slow immersion in liquid N_2 or a pentane/liquid N_2 slush bath.

The EPR spectra were quantitated by double integration of signal-averaged scans, using either a 1.25 mM $CuSO_4$ or a reduced BSPAP sample standard. Sample integrations were corrected for the difference in g-values vs the Cu standard (Aasa & Vänngard, 1975). In all cases, the signals integrated to 0.90 – 1.10 spins/mol of protein, except for the phosphate and AMP samples, which integrated to ca. 0.70 spins/mol of protein. All samples showed a signal just above $g = 2$ due to small (≤20%) and variable amounts of adventitious Cu^{2+}.

The energy difference between the ground state and first excited state levels was estimated by the temperature dependence of the signal. The product of the integrated intensity and temperature was plotted versus temperature, and this plot was fitted to estimate the energy separation between the $S = {}^1/_2$ ground state and the $S = {}^3/_2$ and higher excited states, noting that the separation between the $S = {}^1/_2$ ground state and the $S = {}^3/_2$ first excited state is $3J$ for a coupled ($^5/_2$, 2) system. The procedure of Debrunner (Pearce et al., 1987; Rutter et al., 1984) and Makinen (Yim et al., 1982) involving the measurement of the saturation properties of the signal as a function of temperature was also utilized for selected samples; within experimental error, it gave the same values of J as the simpler temperature dependence method.

The $BSPSP_r$·MoO_4 and ·WO_4 complexes were prepared by adding 15 μL of the inhibitor stock solution (at pH 8.0 to avoid formation of polyoxoanion species) to dilute (ca. 2 mg/mL) $BSPAP_r$ to give a 1:1 ratio of MoO_4 or WO_4 to enzyme, followed by concentration on a Centricon 10 to 16 mg/mL.

Titration of the $BSPAP_r$–fluoride sample was achieved by thawing the sample, adding 15-μL aliquots of a stock NaF solution, and refreezing the sample. During freeze/thaw cycles, typically 5–10% of the sample denatured in the presence of the inhibitor. Signal integrations were corrected for this denaturation as well as the dilution of the sample due to addition of inhibitor.

RESULTS AND DISCUSSION

EPR Spectrum of $BSPAP_r$. Previous work had shown that BSPAP as isolated earlier under low-salt conditions exhibited distinct differences from Uf in properties such as the pH dependence of the EPR spectrum of the reduced enzyme and the optical spectra of oxyanion–enzyme complexes (Averill et al., 1987; Pyrz et al., 1986). These differences were originally attributed to the fact that BSPAP is normally isolated as a complex of two nonidentical subunits [apparently as a result of proteolytic cleavage (Orlando et al., submitted for publication)], while Uf consists of a single polypeptide chain of essentially the same overall molecular weight. Recently, however, the use of high-salt conditions has been demonstrated to yield a highly ordered form of BSPAP with properties much more similar to those of Uf, and the previously observed differences have been attributed to the existence of significant conformational differences between the two forms of BSPAP (Vincent et al., 1991a). Consequently, it was necessary to examine the EPR spectrum of the high-salt form of $BSPAP_r$.

As shown in the top panel of Figure 1, high-salt $BSPAP_r$ at pH 5.0 gives an EPR spectrum that appears to be due to a mixture of two rhombic species, with all g values below 2. This result and the appearance of the spectrum are very similar to those reported for low-salt $BSPAP_r$ and attributed to a pH-dependent mixture of two forms with an apparent pK_a of 4.4 (Averill et al., 1987; Dietrich et al., 1991). The ratio of the two species in Figure 1 differs from that reported previously for high-salt $BSPAP_r$ at pH 5.0 (Vincent et al., 1991a), with the $g = 1.98$ feature and the central zero-crossing feature being significantly more intense. In fact, the spectrum in Figure 1 closely approximates that previously obtained for the low-salt form of $BSPAP_r$ at pH 4.93. The spectrum in Figure 1 is, however, not due to a pH-dependent equilibrium between two species, since it does not change over the pH range 4.25–7.0. The high-salt form of $BSPAP_r$ denatures rapidly at pH ≤ 4.0, preventing examination over a wider pH range. The lack of pH dependence in this range is similar to that reported for Uf_r (Pyrz et al., 1986), although the EPR spectrum of Uf_r does broaden and shift at pH 3.0. Apparent mixtures of two or more species have been previously observed

[2] The abbreviations PO_4, MoO_4, etc. are used without specifying the actual state of protonation of the oxyanion.

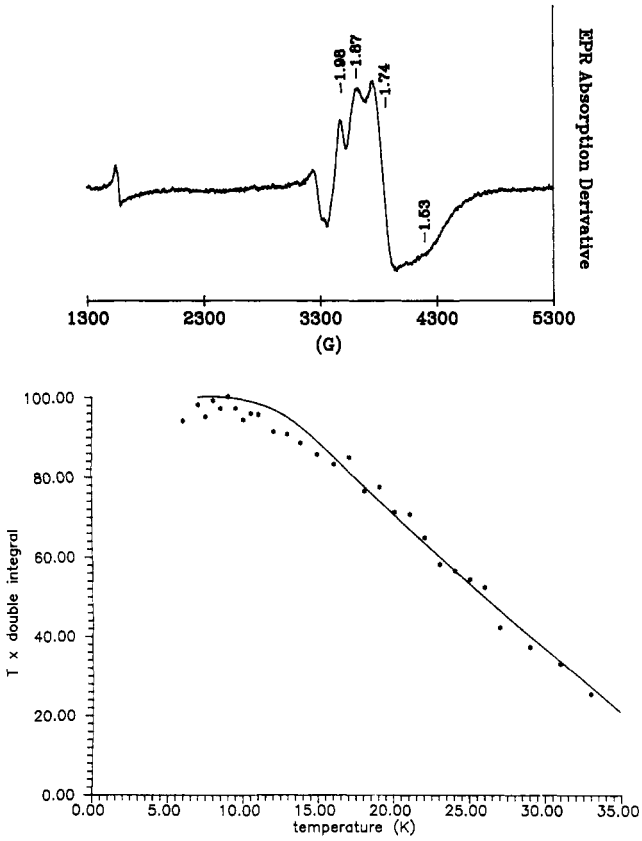

FIGURE 1: (Top panel) EPR spectrum of high-salt BSPAP at pH 5.0 (16 mg/mL) at 4 K. Conditions: microwave frequency, 9.44 GHz, microwave power, 2 mW; modulation frequency, 100 kHz, modulation amplitude, 10 G; time constant, 164 ms; scan time, 335 s; 5 scans; field set, 3750 G; scan range, 2500 G; instrument gain 3200. (Bottom panel) Temperature dependence of the EPR spectrum of high-salt $BSPAP_r$.

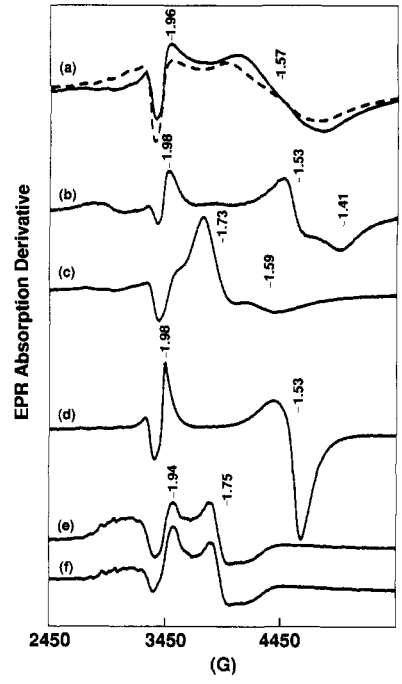

FIGURE 2: (a) EPR spectra of high-salt $BSPAP_r$·AsO_4 at pH 5.0 (solid line) and pH 3.75 (dashed line). Conditions were as described in Figure 1 except for the following: [AsO_4], 1.3 mM; microwave power, 32 mW; field set, 4200 G; scan range, 3500 G. (b) EPR spectrum of high-salt $BSPAP_r$·WO_4 at pH 5.0. Conditions were as in (a) except [WO_4] was 0.4 mM. (c) EPR spectrum of high-salt $BSPAP_r$·F^- at pH 5.0. Conditions were as in (a) except [F^-] was 22 mM and the modulation amplitude was 32 G. (d) EPR spectra of high-salt $BSPAP_r$·MoO_4 at pH 5.0 in the absence (–) and presence (···) of 50 mM PO_4; the spectra are indistinguishable. Conditions were as in (a) except the microwave power was 5 mW. (e) EPR spectrum of high-salt $BSPAP_r$·AMP at pH 5.0. Conditions were as in (a) except [AMP] was 50 mM, microwave power was 100 mW, and the modulation amplitude was 32 G. (f) EPR spectrum of high-salt $BSPAP_r$·PO_4 at pH 5.0. Conditions were as in (e) except [PO_4] was 50 mM.

by EPR for Uf_r (Antanitis & Aisen, 1982a; David & Que, 1990), but these have been attributed to freezing artifacts rather than a simple pH-dependent equilibrium (Antanaitis & Aisen, 1982a).

The temperature dependence of the EPR spectrum of $BSPAP_r$ is illustrated in the bottom panel of Figure 1. Over the range 7–25 K, an exponential decrease in signal intensity is observed as the $S = {}^3/_2$ and higher excited states are populated at the expense of the $S = {}^1/_2$ ground state that gives rise to the signal. A fit of the data to a Boltzmann distribution gave a value of $-2J = 11.0\ cm^{-1}$ (Figure 1, bottom), while a plot of $\ln P_{1/2}$ vs $1/T$ gave a value of $10.8\ cm^{-1}$. These results are consistent with previous findings from EPR (Antanaitis et al., 1983; Averill et al., 1987), NMR (Lauffer et al., 1983), and SQUID magnetization studies (Day et al., 1988) that antiferromagnetic coupling between the ferric and ferrous ions in PAP_r's at pH 5.0 is quite weak ($-2J = 10–25\ cm^{-1}$). In particular, the results for the high-salt and low-salt forms of $BSPAP_r$ are identical.

EPR Spectra of $BSPAP_r$–Oxyanion Complexes. It has previously been demonstrated that tetrahedral oxyanions elicit dramatic changes in the rhombic EPR spectrum of Uf_r (Antanaitis et al., 1983; Antanaitis & Aisen, 1985; David & Que, 1990; Doi et al., 1987; Pyrz et al., 1986). It was shown earlier that addition of MoO_4 or WO_4 to Uf_r produced an axial signal (Antanaitis et al., 1983), while PO_4 and AsO_4 were reported to result in the disappearance of the EPR spectrum, which was attributed to oxidation of the binuclear center even under anaerobic conditions (Antanaitis & Aisen, 1985). Subsequently it was shown that it requires a combination of low temperature (<4 K) and high microwave power for optimal observation of the broad, anisotropic signals of Uf_r·PO_4 and Uf_r·AsO_4 (Day et al., 1988). Direct evidence for coordination of MoO_4 and PO_4 to the binuclear center has also been obtained (Doi et al., 1988b; David & Que, 1990).

As shown in Figure 2, spectra a and d, arsenate and molybdate bind to $BSPAP_r$ to produce broad rhombic and sharp axial spectra, respectively, similar to the analogous complexes of Uf_r. Tungstate produces a slightly rhombic signal very similar to that observed with molybdate (Figure 2b), while AMP and phosphate result in extreme broadening of the spectrum (Figure 2e,f) analogous to that reported for $BSPAP_r$·PO_4 (Dietrich et al. 1991) and Uf_r·PO_4 (Day et al., 1988) at temperatures of ≥4 K. The similarity in the spectra obtained with AMP and phosphate strongly suggests a common mode of binding, consistent with the kinetics results reported earlier (Vincent et al., 1991a). Available instrumentation did not permit access to the 2–3-K temperature range presumed necessary for optimal observation of these signals.

Arsenate has been shown to inhibit BSPAP in a mixed competitive–noncompetitive fashion analogous to that observed with phosphate (Vincent et al., 1991a); analysis of the kinetics data indicated that it has ca. 10-fold greater affinity for the noncompetitive site than does phosphate. The EPR spectrum of $BSPAP_r$·AsO_4 at pH 5.0 (Figure 2a) is virtually identical to that observed for Uf_r·AsO_4 (David & Que, 1990). Lowering the pH to 3.75 results in further broadening of the spectrum (Figure 2a, dashed line), possibly due to protonation of the

bound arsenate, resulting in a binding mode more similar to that of phosphate. Less efficient hydrogen bonding between coordinated arsenate and the putative μ-OH has been postulated previously to account at least in part for the observed differences in spectroscopic properties of Uf_r·PO_4 vs Uf_r·AsO_4 (David & Que, 1990). The observed broadening for BSPAP$_r$·AsO_4 at low pH is consistent with protonation making the bound AsO_4 a better proton donor and hence more like phosphate in this model for oxyanion coordination. The temperature dependence of the BSPAP$_r$·AsO_4 complex at pH 5.0 is consistent with a value of $-2J = 6 \pm 1$ cm^{-1}, which is significantly lower than the 12 ± 1 cm^{-1} value observed for the corresponding Uf_r·AsO_4 species (David & Que, 1990).

Molybdate and tungstate are potent noncompetitive inhibitors of BSPAP with K_i's of ca. 2 μM and 1 μM, respectively (Vincent et al., 1991a). The EPR spectra of the BSPAP$_r$·MoO_4 and BSPAP$_r$·WO_4 complexes are shown in Figure 2, spectra d and b, respectively. The axial spectrum of the former is essentially identical to that of Uf_r·MoO_4 (David & Que, 1990; Day et al., 1988), but the spectrum of the corresponding Uf_r·WO_4 complex has apparently not been published. As might be expected on the basis of the similarity between tungstate and molybdate in inhibition parameters and optical spectral effects (Vincent et al., 1991a), the EPR spectra of the two species are quite similar in shape and position, although the tungstate complex exhibits a small rhombic distortion. Despite the similarities in EPR spectra of the Uf_r·MoO_4 and BSPAP$_r$·MoO_4 complexes, there exists a significant difference in the chemistry of the two species. The Uf_r·MoO_4 complex is reported to be prepared by addition of ca. 1 equiv of Na_2-MoO_4 to a concentrated solution of Uf_r followed by freezing. Initial attempts to prepare the corresponding BSPAP$_r$·MoO_4 complex using the same procedure gave an EPR spectrum that was clearly due to a mixture of BSPAP$_r$·MoO_4 and uncomplexed BSPAP$_r$ in variable but significant proportions (data not shown). Thawing the sample, addition of a second equivalent or excess molybdate, and refreezing did not result in complete formation of the BSPAP$_r$·MoO_4 complex. Since the reported binding constants for molybdate to Uf_r (David & Que, 1990) and BSPAP$_r$ (Vincent et al., 1991a) are both in the 2–4 μM range, we hypothesize that the observed lack of complex formation is due to the fact that, under the conditions used for the BSPAP$_r$ samples (pH 5.0), acid-induced polymerization of molybdate to polyoxomolybdate species is faster than formation of the desired BSPAP$_r$·MoO_4 complex. This complication could be avoided simply by addition of molybdate (or tungstate) to a more dilute protein sample followed by concentration via ultrafiltration. In this regard, it should be noted that an EPR spectrum recently reported for BSPAP$_r$·WO_4 (Dietrich et al., 1991) appears to be the spectrum of a mixture of BSPAP$_r$·WO_4 and uncomplexed BSPAP$_r$, apparently due to a similar problem in sample preparation. The temperature dependence of the EPR signals is consistent with values of $-2J = 8.8$ and 8.0 cm^{-1} for BSPAP$_r$·MoO_4 and BSPAP$_r$·WO_4, respectively.

Evidence for a Ternary BSPAP$_r$·MoO_4·PO_4 Complex. Previous kinetics and spectroscopic studies strongly suggest the existence of two distinct binding sites for tetrahedral oxyanions, one at the substrate binding site to which arsenate and phosphate bind preferentially and one at a different site to which molybdate and tungstate bind exclusively, resulting in noncompetitive inhibition (Vincent et al., 1991a, 1992a). Indeed, it has been suggested that molybdate and tungstate bind to the ferric site to replace a coordinated hydroxide necessary for hydrolysis of the covalent phosphoryl-enzyme

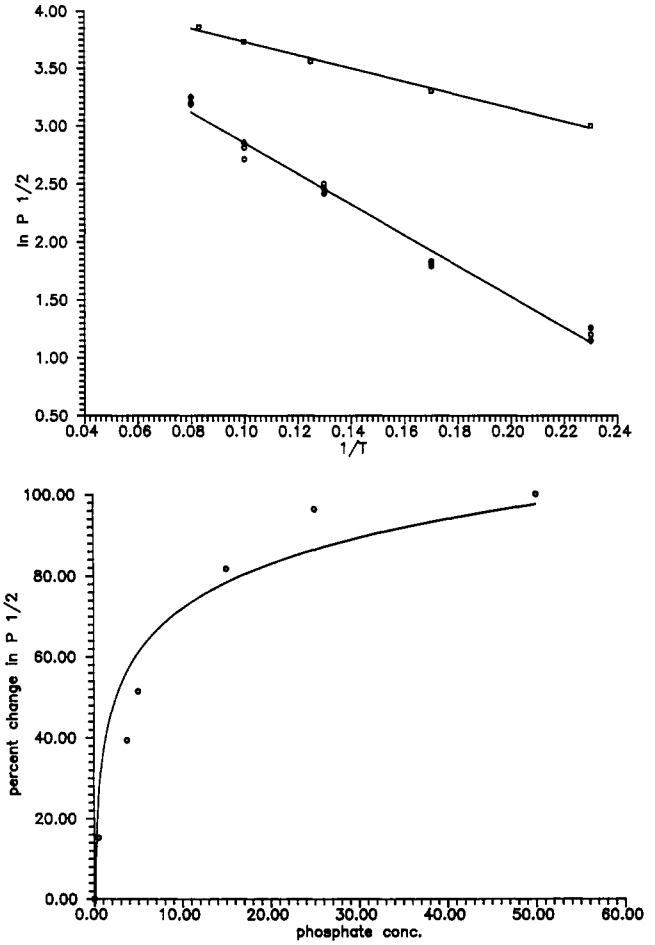

FIGURE 3: (Top panel) Plot of ln $P_{1/2}$ vs $1/T$ for the two samples in Figure 2d. The lower line (BSPAP$_r$·MoO_4 + PO_4) is a best fit to the three sets of data shown; the upper line is a single experiment, but plots of normalized intensity vs temperature (not shown) gave identical results. (Bottom panel) Plot of $\Delta P_{1/2}$ vs [PO_4]. The solid line is the best fit to the dissociation equation in the text, with K_d = 0.5 mM.

intermediate as in structure **1** (Vincent et al., 1992a). If this hypothesis is correct, then it might well be possible to occupy both the oxyanion binding sites simultaneously to produce a ternary species analogous to **1**. It has been previously reported that addition of phosphate to Uf_r·MoO_4 at pH 4.9 resulted in no change in its axial EPR spectrum (Antanaitis & Aisen, 1985), while prolonged incubation (presumably aerobic) resulted in formation of Uf_o·PO_4 (David & Que, 1990).

As shown in Figure 2d, addition of 50 mM phosphate to BSPAP$_r$·MoO_4 also results in no obvious change in the appearance of the axial EPR spectrum. There is, however, a clear change in the power saturation behavior of the sample containing phosphate, which begins to saturate only at 110 mW vs 8 mW for BSPAP$_r$·MoO_4. This suggests a substantially weaker coupling between the iron ions in the phosphate-containing sample, as confirmed by ln $P_{1/2}$ vs $1/T$ plots (Figure 3, top panel), which show that $-2J$ decreases from 8.8 to 4.0 cm^{-1} upon addition of 50 mM phosphate. Finally, as shown in Figure 3, lower panel, the power saturation behavior varies with phosphate concentration in a manner that approximates a protein–ligand binding curve with a K_d of ca. 0.5 mM, which is indistinguishable from the K_d of 0.7 mM calculated for binding of phosphate to the substrate binding site, resulting in competitive inhibition. The clear evidence for saturation of the effect at phosphate concentrations $\geq$50 mM and the fact that the experiment was carried out at high ionic strength

(2 M KCl) make it unlikely that the observed change in microwave power dependence is due to nonspecific effects involving subtle changes in protein conformation. The simplest, and most likely, explanation for the data in Figure 3 is that phosphate is binding to $BSPAP_r \cdot MoO_4$ to yield a ternary complex with weakened antiferromagnetic coupling within the mixed-valence diiron center:

$$BSPAP_r \cdot MoO_4 + P_i \rightleftarrows BSPAP_r \cdot MoO_4 \cdot PO_4$$

It is worth noting that the effect of phosphate binding to both native $BSPAP_r$ and $BSPAP_r \cdot MoO_4$ is to substantially weaken the antiferromagnetic coupling, suggesting a similar mode of phosphate coordination and physical basis for the effect in both cases. It should also be pointed out, however, that the lack of change in the shape of the spectrum is not consistent with the general correlation between increasing g-value anisotropy and decreasing value of $-2J$ observed for Uf_r and its anion complexes (Day, et al., 1988; David, et al., 1990).

Binding of Fluoride to BSPAP$_r$. It has been previously reported that fluoride exhibits unusual behavior as an inhibitor of BSPAP, resulting in curvilinear Lineweaver–Burk plots (Davis et al., 1981; Vincent et al., 1991a), and similar results have been obtained for Uf (Ketchum et al., 1985). These results have been interpreted as suggesting that two forms of the enzyme are present, which differ greatly in the degree to which they are inhibited by fluoride (Vincent et al., 1991a). Spectroscopic studies on the effects of fluoride binding are limited, however. Excess fluoride has been shown to shift the visible maximum of Uf_r from 510 to 550 nm over a 24-h period, resulting in complete loss of the rhombic EPR signal, which was attributed to fluoride-induced aerobic oxidation (Antanaitis & Aisen, 1985). In contrast, addition of fluoride to the high-salt form of $BSPAP_r$ and $BSPAP_o$ was reported to result in blue shifts of 18 and 30 nm, respectively (Vincent et al., 1991a), suggesting that fluoride coordinates to the binuclear iron center.

As shown in Figure 2c, addition of 22 mM fluoride to $BSPAP_r$ results in a new EPR spectrum, with a minimum at $g = 1.59$ and a crossover point at $g = 1.73$. The appearance of the spectrum strongly suggests a reversal of the principal components of the g-tensor such that g_z occurs at high field, rather than at low field as observed for all other PAP_r species. The signal intensity remained constant at 0.85–0.90 spins/molecule upon standing for 24 h at 4 °C. The signal did not change in shape or intensity when the fluoride concentration was increased to >100 mM. This result strongly indicates that fluoride binds to the binuclear center, perhaps by replacing a coordinated water or the coordinated hydroxide postulated to be necessary for hydrolysis of the covalent phosphoryl-enzyme intermediate (Vincent et al., 1992a,b). This is similar to the proposed mode of inhibition of BSPAP by tetrahedral oxyanions such as molybdate and tungstate (Vincent et al., 1992a). Unlike the oxyanions, however, coordinated fluoride might be able to participate in the catalytic mechanism to produce an alternative product, fluorophosphate. Although its formation is plausible, we have been unable to detect fluorophosphate in solution using ^{19}F NMR (M. W. Crowder and B. A. Averill, unpublished results); however, the expected rate of hydrolysis of the fluoride-bound species along with the rapid hydrolysis of fluoride from FPO_3 in water may have resulted in low levels of the product, thereby precluding detection by NMR.

CONCLUSIONS

Tetrahedral oxyanions have been shown to bind to the mixed-valence binuclear iron center of $BSPAP_r$, producing characteristic changes in the EPR spectrum. The spectral data are summarized in Table I and compared to available data for corresponding complexes of Uf_r. In general, there is excellent agreement between the g-values for corresponding derivatives of $BSPAP_r$ and Uf_r, but the calculated values of $-2J$ for former are generally smaller by 40–50%. The fact that ^1H NMR spectra of $BSPAP_r$ generally show significantly broader lines than are observed for Uf_r (Wang et al., 1992) suggests that differences in relaxation properties between the two systems are real. The present results, with a larger variety of anions than previously examined, also call into question the previously postulated correlation between g-value anisotropy and the magnitude of $-2J$ (David & Que, 1990). The grouping of oxyanions on the basic of their inhibition behavior and effects on the visible absorption spectrum of the enzyme (Vincent et al., 1991a) is reinforced by the EPR data (Table I). Phosphate, AMP, and arsenate all result in broadened EPR spectra with decreased values of $-2J$, while molybdate and tungstate result in sharp axial and slightly rhombic spectra, respectively, and fluoride produces an anomalous spectrum with an inverted g-tensor. These results are consistent with binding of the two classes of oxyanions to distinct sites at or near the binuclear center, while fluoride binds in yet a third mode. The conclusion about two classes of oxyanion binding sites is reinforced by data suggesting that phosphate can bind to the $BSPAP_r \cdot MoO_4$ complex, resulting in a decrease in $-2J$ as observed for the binary $BSPSP_r \cdot PO_4$ complex. ENDOR and EXAFS experiments to confirm the existence of the putative ternary $BSPAP_r \cdot MoO_4$ complex are in progress.

Table I: EPR Spectral Features and $-2J$ Values for Anion Complexes of $BSPAP_r$ and Uf_r

form	EPR g-values[a]	$-2J$ (cm^{-1})
$BSPAP_r$	1.98, 1.87, 1.74, 1.53[b]	11.0[b]
Uf_r	1.96, 1.74, 1.56[c]	19.8[c], 20[d]
$BSPAP_r \cdot AMP$	1.94, 1.75[b]	6.0[b]
$BSPAP_r \cdot PO_4$	1.94, 1.75[b]	6.0[b]
$Uf_r \cdot PO_4$	2.27, 1.51, 1.06[c]	6.0[c]
$BSPAP_r \cdot AsO_4$	1.97, 1.57[b]	6.0[b]
$Uf_r \cdot AsO_4$	1.92, 1.56, 1.41[e]	12[e]
$BSPAP_r \cdot MoO_4$	1.98, 1.53[b]	8.8[b]
$Uf_r \cdot MoO_4$	1.97, 1.52[c]	15[e], 20[f]
$BSPAP_r \cdot WO_4$	1.98, 1.53, 1.41[b]	8.0[b]
$BSPAP_r \cdot MoO_4 \cdot PO_4$	1.98, 1.53[b]	4.0[b]
$BSPAP_r \cdot F^-$	1.73, 1.59[b]	3.4[b]

[a] Apparent g-values estimated from the EPR spectrum except for the Uf_r and $Uf_r \cdot MoO_4$ data, which were derived by fitting the spectra. [b] This work. [c] Day et al., 1988. [d] Lauffer et al., 1983. [e] David & Que, 1990. [f] Scarrow et al., 1990.

REFERENCES

Aasa, R., & Vänngard, T. (1975) *J. Magn. Reson. 19*, 308–315.

Antanaitis, B. C., & Aisen, P. (1982a) *J. Biol. Chem. 257*, 1855–1859.

Antanaitis, B. C., & Aisen, P. (1982b) *J. Biol. Chem. 257*, 5330–5332.

Antanaitis, B. C., & Aisen, P. (1983) *Adv. Inorg. Biochem. 5*, 111–136.

Antanaitis, B. C., & Aisen, P. (1985) *J. Biol. Chem. 260*, 751–756.

Antanaitis, B. C., Strekas, T., & Aisen, P. (1982) *J. Biol. Chem. 257*, 3766–3770.

Antanaitis, B. C., Aisen, P., & Lilienthal, H. R. (1983) *J. Biol. Chem. 258*, 3166–3172.

Averill, B. A., Davis, J. C., Burman, S., Zirino, T., Sanders-Loehr, J., Loehr, T., Sage, J. T., & DeBrunner, P. (1987) *J. Am. Chem. Soc. 109*, 3760–3767.

Burman, S., Davis, J. C., Weber, M. J., & Averill, B. A. (1986) *Biochem. Biophys. Res. Commun. 136*, 490–497.

David, S. S., & Que, L., Jr. (1990) *J. Am. Chem. Soc. 112*, 6455–6463.
Davis, J. C., & Averill, B. A. (1982) *Proc. Natl. Acad. Sci. U.S.A. 79*, 4623–4627.
Davis, J. C., Lin, S. S., & Averill, B. A. (1981) *Biochemistry 20*, 4062–4067.
Day, E. P., David, S. S., Peterson, J., Dunham, W. R., Bonvoisin, J. J., Sands, R. H., & Que, L., Jr. (1988) *J. Biol. Chem. 263*, 15561–15567.
Debrunner, P. G., Hendrich, M. P., DeJersey, J., Keough, D. T., Sage, J. T., & Zerner, B. (1983) *Biochim. Biophys. Acta 745*, 103–106.
Dietrich, M., Munstermann, D., Suerbaum, H., & Witzel, H. (1991) *Eur. J. Biochem. 199*, 105–113.
Doi, K., Antanaitis, B. C., & Aisen, P. (1986) *J. Biol. Chem. 261*, 14936–14938.
Doi, K., Gupta, R., & Aisen, P. (1987) *J. Biol. Chem. 262*, 6982–6985.
Doi, K., Antanaitis, B. C., & Aisen, P. (1988a) *Struct. Bonding 70*, 1–26.
Doi, K., McCracken, J., Peisach, J., & Aisen, P. (1988b) *J. Biol. Chem. 263*, 5757–5763.
Gaber, B. P., Sheridan, J. P., Bazer, F. W., & Roberts, R. M. (1979) *J. Biol. Chem. 254*, 8340–8342.
Kauzlarich, S. M., Teo, B. K., Zirino, T., Burman, S., Davis, J. C., & Averill, B. A. (1986) *Inorg. Chem. 25*, 2781–2785.
Ketchum, C. M., Baumbach, G. A., Bazer, F. W., & Roberts, R. M. (1985) *J. Biol. Chem. 260*, 5768–5776.
Lauffer, R. B., Antanaitis, B. C., Aisen, P., & Que, L., Jr. (1983) *J. Biol. Chem. 258*, 14212–14218.
Mockler, G. M., deJersey, J., Zerner, B., O'Connor, C. J., & Sinn, E. (1983) *J. Am. Chem. Soc. 105*, 1891–1893.
Pearce, L. L., Kurtz, D. M., Xia, Y.-M., & Debrunner, P. G. (1987) *J. Am. Chem. Soc. 109*, 7286–7293.
Pyrz, J. W., Sage, J. T., DeBrunner, P. G., & Que, L., Jr. (1986) *J. Biol. Chem. 261*, 11015–11020.
Que, L., Jr., & Scarrow, R. C. (1988) Metal Clusters in Proteins, ACS Symposium Series 38, pp 152–178, American Chemical Society, Washington, CD.
Que, L., Jr., & True, A. E. (1990) *Prog. Inorg. Chem. 38*, 97–200.
Rutter, R., Hager, L. P., Dhonau, H., Hendrich, M., Valentine, M., & Debrunner, P. G. (1984) *Biochemistry 23*, 6809–6816.
Scarrow, R. C., Pryz, J. W., & Que, L., Jr. (1990) *J. Am. Chem. Soc. 112*, 657–665.
Sinn, E., O'Connor, C. J., DeJersey, J., & Zerner, B. (1983) *Inorg. Chim. Acta 78*, L13–L15.
Vincent, J. B., & Averill, B. A. (1990) *FASEB J. 4*, 3009–3014.
Vincent, J. B., Olivier-Lilley, G. L., & Averill, B. A (1990) *Chem. Rev. 90*, 1447–1467.
Vincent, J. B., Crowder, M. W., & Averill, B. A. (1991a) *Biochemistry 30*, 3025–3034.
Vincent, J. B., Crowder, M. W., & Averill, B. A. (1991b) *J. Biol. Chem. 266*, 17737–17740.
Vincent, J. B., Crowder, M. W., & Averill, B. A. (1992a) *Biochemistry 31*, 3033–3037.
Vincent, J. B., Crowder, M. W., & Averill, B. A. (1992b) *Trends Biochem. Sci. 17*, 105–110.
Wang, D. L., Holz, R. C., David, S. S., Que, L., Jr., & Stankovich, M. T. (1991) *Biochemistry 30*, 8187–8194.
Wang, Z., Ming, L.-J., Que, L., Jr., Vincent, J. B., Crowder, M. W., & Averill, B. A. (1992) *Biochemistry 31*, 5263–5268.
Yim, M. B., Kuo, L. C., & Makinen, M. W. (1982) *J. Magn. Reson. 46*, 247–256.